Title

A highly integrated precision nanomedicine strategy to target esophageal squamous cell cancer molecularly and physically

Authors

Wang, Xin-Shuai
Ding, Xue-Zhen
Li, Xiao-Cen
et al.

Peer reviewed

A Highly Integrated Precision Nanomedicine Strategy to Target Esophageal Squamous Cell Cancer Molecularly and Physically

Xin-shuai WANG[1], **Xue-zhen DING**[1], **Xiao-cen LI**[2], **Yixuan HE**[2], **De-jiu KONG**[1], **Li ZHANG**[1], **Xiao-chen HU**[1], **Jun-qiang YANG**[1], **Meng-qi ZHAO**[1], **She-gan GAO**[1,*], **Tzu-yin LIN**[3,*], **Yuanpei LI**[2,*]

[1]Henan Key Laboratory of Cancer Epigenetics; Cancer hospital, The First Affiliated Hospital, College of Clinical Medicine, Medical College of Henan University of Science and Technology, Luoyang, China, 471003

[2]Department of Biochemistry & Molecular Medicine,

[3]Department of Internal Medicine, UC Davis Comprehensive Cancer Center, University of California Davis, Sacramento, CA 95817, USA

Abstract

The prognosis of esophageal squamous cell carcinoma is very poor. We firstly identified PI3K overexpression in patient samples and its relation to poor patient survival. With our highly versatile disulfide cross-linked micelle (DCM) based tumor-targeted drug delivery platform, we were able to load a potent but toxic docetaxel (DTX) and another clinical stage PI3K inhibitor (AZD8186) with favorable physical properties, including small size and high loading efficiency. The combination of the DTX-DCM and AZD8186-DCM showed a highly efficacious and synergistic anti-tumor effect and decreased hematotoxicity. A pro-apoptotic protein, Bax was significantly upregulated in ESCC cells treated with combination therapy compared to that with monotherapy. In conclusion, this study utilized a highly integrated precision nano-medicine strategy that combines the identification of cancer molecular target from human patients, precision drug delivery and effective combination therapy for the development of better ESCC treatment.

Keywords

Introduction

Esophageal squamous cell carcinoma (ESCC) remains significant health challenges around the world, with an estimated 482,300 newly diagnosed cases and 406,800 ESCC related

deaths each year [1]. The incidence of ESCC is increasing, while the prognosis is extremely poor [2]. The 5-year survival rate of patients with esophageal cancer rarely exceeds 40% [3]. Local recurrence after initial treatment is the major cause of treatment failure in the patients[4, 5]. Treatment with curative intent involves either resection with or without neoadjuvant therapy, or definitive chemoradiotherapy with or without salvage resection [6]. The major limitation of chemotherapy includes a lack of specificity that results in low concentrations of chemotherapeutic drugs/agents at tumor sites, along with severe off-target toxic effects [7]. Therefore, there is an urgent critical need for new therapies and more effective strategies to enhance the curative effect and reduce the toxicities.

Molecularly targeted therapy has been an emerging trend for practicing precision medicine. Dysregulation of PI3K has been identified in several solid tumors, such as breast cancer, prostate cancer, including esophageal cancer[8–11]. However, the understanding of the role of PI3K in ESCC is limited. Basic molecular biologists revealed that the suppression of esophageal tumor growth and chemoresistance could be achieved by targeting the PI3K/AKT pathway[12–14]. AZD8186, a novel small-molecule inhibitor of PI3Kβ and PI3Kδ inhibits the growth of tumor cells, regulating signaling through the PI3K/AKT signaling pathway[15]. AZD8186 is currently in the phase I clinical trial and already showed its promising anti-cancer activity as monotherapy or in combination with docetaxel (DTX) or androgen therapy against prostate cancer, breast cancer, T-cell acute lymphoblastic leukemia[16–18] DTX, a second-generation taxoid, is considered one of the most potent chemotherapeutic agents in the clinical setting[19] that is broadly indicated for the treatment of non-small cell lung cancer, breast cancer, ovary cancer, prostate cancer, stomach cancer, head and neck cancer and esophageal cancer [20, 21]. However, similar to other lipophilic chemotherapy agents, it has major limitations including a lack of specificity that results in low concentrations of chemotherapeutic drugs/agents at tumor sites, along with severe off-target toxic effects [7]. Recently, to overcome these problems and improve anticancer effects, much attention has been focused on the design of nanometer drug delivery platform.

Nanotechnology-based drug delivery platforms offer several distinct advantages for cancer therapy[22–24], such as improved drug solubility, minimal drug leakage during transit to the target, prevention of degradation and premature clearance of the drug, prolonged *in vivo* circulation time and preferential accumulation at tumor site via the enhanced permeability and retention effect, biocompatibility and biodegradability of nanoplatforms. Our group had developed the reversible disulfide cross-linked micelles (DCMs) [25] that could minimize the premature release of drugs from carriers during circulation in the bloodstream and control the release rate of the entrapped drugs at the tumor sites [26]. We already demonstrated that DCM could greatly enhance chemotherapeutic drug efficacy and safety[26]. In this study, we introduced a highly integrated precision nanomedicine strategy that was able target ESCC at both molecluar and physical level. We firstly identified the correlation between PI3K expression levels and ESCC patient survival. We then employed DCMs as a tumor-specific targeting strategy to deliver the molecular target inhibitor (AZD8186) and potent DTX to tumors in mouse model. Our study firstly demonstrated the synergistic effects *in vitro* and *in vivo* of AZD8186 and DTX within nano-formulations against ESCC and greatly reduced hematotoxicity.

Methods

Materials

DTX and AZD8186 was purchased from AK Scientific Inc. (Mountain View, CA, USA). 11,1'-Dioctadecyl-3,3,3',3'-etramethylindotricarbocyanineiodide(DiD), a near-infrared dye, was purchased from Biotium (Invitrogen, USA). Annexin V and propidium iodide (PI) were obtained from (Pharmingen, San Diego, CA, USA). Esophageal cancer cell line KYSE70 was obtained from the American Type Culture Collection (ATCC, Manassas, VA). Antibodies for PI3Kfor IHC, pPI3KpAKT(T308), p53(DO-1), Bcl2, Bax (2D2) and β-actin were purchased from Millipore (Massachusetts, USA). Cholic acid, MTS [3-(4, 5-dimethyldiazol-2-yl)-2,5 diphenyl tetrazolium bromide] and all other chemicals were purchased from Sigma-Aldrich (St. Louis, USA) and used as received.

Immunohistochemistry

Expression of PI3K was examined using tumor samples (T) and para-tumor tissue (N) obtained from 60 patients who were diagnosed to have esophageal cancer and treated in the Department of surgical oncology, The First Affiliated Hospital of Henan University of Science and Technology between February 2012 and March 2014. The median age of the patients was 61 years, with a range of 42–79 years. The clinical characteristic of the patients is shown in Table 1.

A standard immunohistochemistry on PI3K staining was performed using a Ventana BenchMark XT immunostainer (Ventana Medical Systems, Tucson, USA) All slides were examined independently and blindly by two senior pathologists. Every tumor was assessed by a score according to the predominant intensity of the cytoplasmic staining (no staining = 0, weak staining = 1, moderate staining = 2, strong staining = 3) and the extent of stained cells (0% = 0, 1–30% = 1, 30–60% = 2, 60–100% = 3). The scores ranged from 0 to 6. The score was 0–1, 2–3 and 4–6 indicating negative expression, middle expression, and positive expression, respectively.

Western blot and quantitative real-time PCR (qRT-PCR)

Protein samples were collected from tumor tissue and paired adjacent normal tissue of postoperative specimens from the 60 esophageal cancer patients. Western blot analysis was used to detect the expression of PI3K in esophageal cancer tissues and adjacent tissues, using antibodies against PI3K and β-actin. Western blot analysis was performed in triplicates and representative blots are depicted.

Total RNA was isolated from tumor tissue and paired adjacent normal tissue of postoperative specimens from the 60 esophageal cancer patients. Then, RNA was reversely transcribed into cDNA. qRT-PCR was used for quantitative cDNA level to detect the expression level of PI3K. In the esophageal cancer tissues, the cut off value of PI3K expression level defined as 5, (the high expression:> 5, the low expression: <5).

Synthesis and Characterizations of AZD8186-DCMs and DTX-DCMs

The PEG_{5k}-Cys_4-L_8-CA_8 telodendrimer, the building block for DCMs was synthesized according to the previous studies [27] by the liquid phase condensation reaction MeO-PEG-NH_2 utilizing stepwise peptide chemistry according to previous published methods [28]. AZD8186-DCMs (1 mg drug in 20 mg PEG_{5k}-Cys_4-L_8-CA_8 telodendrimer) were prepared by the solvent evaporation method as reported previously[29]. The micelle solution was also filtered through a 0.22-μm filter to sterilize the sample.

The size of AZD8186-DCMs and DTX-DCMs (drug-DCMs) were measured by dynamic light scattering (DLS). Transmission electron microscope (TEM, Philips CM-120, Amsterdam, Netherland) was used to observe the morphology of drug-DCMs The amount of drug loaded in the micelles was analyzed by an HPLC system (Waters). The drug-loading efficiency was calculated according to the calibration curve between the HPLC area values and concentrations of the drug standard sample.

Confocal imaging study

The esophageal cancer cell line KYSE70 was cultured in RPMI-1640 medium containing 10% fetal bovine serum (FBS) and penicillin-streptomycin. For cell uptake study, KYSE70 cells were seeded in eight-well tissue culture chamber slides (BD Biosciences, Bedford, MA, USA) and were incubated with 50 μg/ml DID, DID-DCMs, DID-AZD8186-DCMs or DID-DTX-DCMs for 4 hours. Confocal imaging was acquired by LSM 800 (Zeiss, Jena, Germany).

Flow cytometry for cell apoptosis and cell cycle evaluation

Annexin V and propidium iodide (PI) double staining (Pharmingen, San Diego, CA, USA) were used to evaluate the KYSE70 cell apoptosis treated with free DTX, AZD8186, DTX-DCMs, and AZD8186-DCMs. In short, 1×10^6 KYSE70 cells were seeded into two 6-well plates overnight. Cells were treated with various concentrations (3μg/ml, 30μg/ml) of free DTX, free AZD8186, DTX-DCMs, and AZD8186-DCMs for 24h respectively. Cells were harvested and stained with 10μg/ml AnnexinV-FITC and propidium iodide (PI). Similarly, for cell cycle analysis, cells with the same treatment settings were harvested and fixed with 70% cold ethanol at 24h post drug treatment. Cells were stained with 50μg/ml PI and 100μg/ml RNase A (Sigma-Aldrich) and were protected from light. Both samples were evaluated by flow cytometer (Becton–Dickinson, Mansfield, MA, USA), and results were analysed by Flow Jo v7.6.1 software (Tree Star Inc., San Carlos, CA)

Cell viability assay

Cells were plated in 96-well plates (5×10^3/well) overnight and treated with various concentrations of drugs as indicated for another 72h. MTS working solutions were added in each well and incubated for another 4 hours before the plate reading(SpectraMax M2, Molecular Devices, USA). The results are shown as the average cell viability [(re$_{treat}$ −OD_{blank})/($OD_{control}$−OD_{blank})×100%] of triplicate wells.

Western blot

After treatments by free AZD8186, free DTX, AZD8186-DCMs and DTX-DCMs, equal amounts of cell lysate proteins (25μg) were subjected to standard western blot analysis. The transferred membranes were incubated with the appropriate primary antibodies including pPI3K, pAkt, p53, Bcl2, Bax, and β-actin (Millipore Sigma) at 4°C overnight followed by secondary antibody. The level of proteins was quantified using Quantity One software (BioRad, USA)

Near-infrared fluorescence imaging study in ESCC xenograft-bearing mouse

Animals were acclimatized in the holding facility prior to the study. All animal procedures were approved by the Animal Use and Care Administrative Advisory Committee at the University of California, Davis. Xenograft model was established by injecting 7×10^6 KYSE70 esophageal cancer cells in a 100μL of a mixture of PBS and Matrigel (1:1 v/v) subcutaneously into the left flank of nude mice (Harland). When the tumor volume reached approximately 8~10 mm diameter, they were subjected to *in vivo* NIRF optical imaging. At different time points post-injection of DiD-AZD8186- DCMs (DiD 50 mg/kg; AZD8186 10 mg/kg), The mice were then scanned with Kodak multimodal imaging system IS2000MM with an excitation bandpass filter at 625nm and an emission at 700nm. Twenty-four hours after administration, mice were humanely euthanized and major organs and tumors were collected for *ex vivo* imaging.

Efficacy study in xenograft mouse model

KYSE70 esophageal cancer cells xenograft-bearing nude mice were used to evaluate the therapeutic efficacy. After the tumor volume reached about 100 mm^3, mice were randomized into 6 groups (n=8 per group): free DTX (5mg/kg), DTX-DCMs (5mg/kg), free AZD8186(10mg/kg), AZD8186-DCMs (10mg/kg), and AZD8186-DTX-DCMs (DTX 5mg/kg and AZD8186 10mg/kg), respectively every three days. All treatments were given *via* tail vein except free AZD 8186 was given via gavage every day for a total of 21 days. The tumor volumes were measured every three days to assess the antitumor activities of the treatments, and the body weights were examined to monitor potential toxicity. Tumor volume was calculated by the formula (L×W2)/2, where L is the longest and W is the shortest in tumor diameters (mm). All animals were sacrificed on day 21, and all tumors were collected for photo imaging and weighing. Blood samples were obtained 1day after the first dose for measurement of complete blood count (CBC) and analysis of serum biochemistry. ***Statistical analysis***

Data were expressed as the mean ± standard error (SEM) unless otherwise noted Statistical analysis was performed by Student's t-test for two groups, and one-way ANOVA for multiple groups. A p-value of less than 0.05 was considered statistically significant. Kaplan-Meier is used for survival analysis.

Results

Correlation of PI3Kexpression level with esophageal cancer patient survival

To examine the possible roles of PI3K expression in ESCC patients, tumor samples surgically resected from 60 esophageal cancer patients were examined for the expression of these molecules using qRT-PCR(Fig 1A), IHC (Fig 1B), and western blot (Fig 1C). The mean age of the 63 patients was 62 years, 15 patients were positive for lymph nodes and 45 patients were negative, 44 patients were in clinical stageI-II, and 16 were in stageIII. Quantitative Real-time PCR analysis was performed to determine the cDNA level to detect the expression level of PI3K in 60 pairs of esophageal cancer tissue and adjacent tissue specimens. We found that the expression of PI3K in tumor tissues was conspicuously higher than that of the adjacent tissues ($P < 0.05$, Fig 1A). We further performed the IHC analysis on those patient sample tissue sections and revealed that PI3K had a cytoplasmic staining pattern. Among 60 patients, 28 patients (account for 46.7%) were considered as high expression and 20 patients (33.3%) as low expression (Fig 1B) based on our scoring system based on PI3K staining intensity. Consistent with the qRT-PCR results, the expression of PI3K in esophageal cancer tissues was significantly higher than that in adjacent tissues (Fig 1C).

Patients with clinical follow-up were evaluated with respect to the association of immunostaining scores tooverall survival (OS). OS was defined as the date of diagnosis to death of any cause or to the date of the last visit. The Kaplan-Meier survival analysis showed that there was significant statistically difference in 30 months OS between the patients with PI3K low expression and PI3K high expression (HR=2.192, 95% CI 1.07 to 4.49, $P = 0.0319$) (Fig 1D), revealing that the expression of PI3K is a significant predictive factor for OS in patients with esophageal cancer treated with surgery.

Synthesis and Characterization of AZD8186-DCMs and DTX-DCMs

There are many challenges in co-delivery of molecularly targeted drugs and chemotherapeutic drugs to the target tumor sites, such as the determination of drug ratio, treatment regimen (concurrence or sequential, and frequency), and potential for various combinations. Therefore, we decided to provide more flexibility by loading two drugs separately for our study. As previously described [30], we successfully loaded AZD8186 and DTX in disulfide cross-linked micelles (DCMs) to prepare AZD8186-DCMs and DTX-DCMs. The average particle size of AZD8186-DCMs and DTX-DCMs were 20± 6 nm and 21± 7 nm, respectively (Fig 2A). Both micelles were spherical in shape with a size that was consistent with the result obtained from the DLS particle sizer (Fig 2A). The drug loading efficiency of AZD8186 and DTX was 85.2% and 82.4%, respectively, based the HPLC measurements.

To investigate intracellular uptake behavior of AZD8186-DCMs and DTX-DCMs, we further co-loaded DiD as a fluorescence marker and incubated with ESCC cell line, KYSE70. Figure 2C demonstrated that DiD-AZD8186-DCMs and DiD-DTX-DCMs were both successfully internalize into KYSE70 cells with a cytoplasmic pattern only after 2h of incubation (Fig 2B).

In vitro anti-cancer efficacy studies in KYSE70 cell line

After confirmation of the cellular uptake of nanopartilces, we further researched their anti-cancer efficacy in ESCC cell line. Cells were treated with both free and DCM formulated drugs, and cell viability, cell apoptosis, and cell cycle distribution were evaluated. Both free and DCM-AZD8186 effectively caused a dose-dependent loss in cell viability due to induction of cell apoptosis (including increases of early (Annexin+/PI-) and late (Annexin +/PI+) apoptosis) and G1 arrest (increased G1 % compared to control) (Fig 3 A,B,C & Fig S1). In contrast, KYSE70 cells were more resistant to DTX and DTX-DCMs treatments, comparing to AZD8186, evidenced by increased IC_{50} and a lesser degree of apoptosis (Fig 3A,B,D, & E). As expected, a significant G2 arrest was observed after DTX treatments (Fig 3 F & Fig S2), as DTX suppressed the dynamics of microtubules resulting in failure in mitosis[31]. Combining with the finding in Fig 2B, these results indicated that AZD8186-DCMs and DTX-DCMs could be uptake by the cells and released to function as anti-cancer agents comparable with their free formulations.

Synergistic effects of AZD8186-DCMs and DTX-DCMs in esophageal cancer

Upon confirming both formulations still kept their pharmacological activity, we next examined the combination effects of various drug ratios, concentrations, and treatment regimens. Given the high PIK3CA gene amplification and PI3K protein expression, KYSE70 cells were selected for our study for targeted therapy[33]. When combing 12.5 or 25 mg/ml of DTX-DCM with various concentrations of AZD8186-DCM, there was a significant synergistic anti-ESCC cancer effect especially at the lower AZD8186 concentrations (Combination Index, CI = 0.2 – 0.9, CI < 1 indicated synergism) (Fig 4A). Similarly, when treating cells with 1.56, 3.125, and 6.25 mg/ml of AZD8186-DCM with various concentrations of DTX-DCM, a slight synergistic effect also only occurred at the lower DTX-DCM concentrations (CI = 0.7–0.9) (Fig S3). Later, we took a different approach to further confirm the synergistic effects using fixed-dose strategy. As shown in the Fig 4B, we utilized different fixed ratios of AZD8186-DCM and DTX-DCM with different concentrations. We demonstrated that AZD8186-DCM and DTX-DCM showed a better synergistic effect at the 1:1 and 2:1 ratios. The ratios of 1:2, 1:5, and 5:1 only had slight synergistic effects. Based on this study, the synergistic effects of AZD8186-DCMs and DTX-DCMs in esophageal cancers were demonstrated.

Several studies demonstrated that the sequence for giving molecular targeting drugs and chemotherapeutic drugs may achieve dramatic different efficacy[34, 35]. Therefore, we intended to study the potential effects of the drug treatment sequence on the anti-ESCC functions. KYSE70 cells were treated with different concentrations of DTX-DCM and AZD8186-DCM concurrently, or in different sequences (DTX-DCM first followed by AZD8186-DCM or in the reverse order). Fig 4C demonstrated that concurrent and sequential treatments (either order) exhibited synergistic effects, while concurrent treatment was significantly more effective than sequential therapy (p<0.05). Consequently, we decided to employ the concurrent treatment regimen in the following animal studies.

Combination therapy with AZD8186-DCM and DTX-DCM effectively inhibited ESCC growth with decreased toxicity

Our previous study already confirmed the superior tumor targeting efficacy of our precision drug delivery platforms in several tumor types, such as prostate cancer, bladder cancer, and ovarian cancer[27, 29]. The present study was our first time to assess the drug delivery specificity and efficiency of DCM platform in ESCC xenograft mouse model. We evaluated the nanoparticle distribution tracking the fluorescence signals from the co-loaded near-infrared dye DiD. KYSE70 cell xenograft-bearing mice were injected with DiD-AZD8186-DCMs and the whole body NIRF imaging was acquired at different time points upon administration. DiD signals were found to gradually accumulate into tumor site and reached the peak at 24h (Fig 5A). All organs and tumors were harvested for *ex vivo* imaging which then showed that DiD-AZD8186-DCMs preferentially accumulated at the tumor sites. However, there were also moderate degrees of the DiD signals identified in the lung, spleen, and liver. Nevertheless, accordingly to our experiences, the DiD signals tend to retain longer in the tumor sites, while declined rapidly in other major organs.

For the *in vivo* antitumor efficacy studies, KYSE70 xenograft-bearing nude mice were treated with PBS, free AZD8186, AZD8186-DCMs, free DTX, DTX-DCMs, or AZD8186-DCMs + DTX-DCMs. The therapeutic effect was evaluated by the changes in tumor size. Compared to PBS control, free DTX and AZD8186 displayed mild inhibition effects on tumor growth, while AZD8186-DCMs and DTX-DCMs showed moderate inhibition effects (Fig 5B&C). DCM formulation treatment groups had significantly lighter tumors compared to free formulation treatment groups (Fig 5C). Moreover, the combination of AZD8186-DCMs and DTX-DCMs demonstrated the most potency in inhibition of ESCC tumor growth than mono-therapy in both formulations (Fig 5B and C). Collectively, this study demonstrated that AZD8186 in combination with docetaxel may result in tumor regression or stasis in esophageal cancer.

General toxicity was assessed by the body weight changes during treatment, and there was no significant difference between treatment groups (Fig 5D). These results supported that nano-formulations itself did not cause or enhance drug-related toxicity. Blood was also collected on the day 2 after the treatment for complete blood count and biochemistry (hepatic and renal function panel) evaluations. Hepatotoxicity and hematologic toxicity are two major side effects of traditional chemotherapy that often lead to early termination of chemotherapy[32, 36, 37]. Compared to PBS control group, there was a significant decrease in the white blood cell count upon free DTX treatment, but not DTX-DCMs or the combination treatment (Table 2). Significant decreases in red blood cell count and hemoglobin concentrations were also identified in the free DTX treated mice comparing to DTX-DCMs and the combination treated groups (Table 2). This result strongly suggested that DCM could significantly decrease bone marrow suppression (inhibition of both RBC and WBC) induced by DTX. This was most likely because DCM could prevent premature drug release during circulation and specifically deliver a higher dose of the chemotherapeutic drug to the tumor sites resulting decreased toxicity. Additionally, there was no obvious liver and renal toxicity evidenced by no significant changes in the serum plasma aspartate aminotransferase (AST), alanine aminotransferase (ALT) levels (both

reflect liver function) and creatinine/urea levels (both reflect kidney function) compared with the control group, and all the parameters were within the normal ranges (Table 3).

Molecular mechanism study

We further elucidated the molecular mechanism for the synergistic anti-tumor efficacy of DTX-DCM and AZD8186-DCM in ESCC cells. AZD8186 is an isoform-specific small-molecule PI3K inhibitor and could block PI3K/Akt signaling pathway [15]. As expected, both free AZD8186 and AZD8186-DCM significantly diminished phosphorylation of both PI3K and Akt ($p < 0.05$). Interestingly, p53, a key tumor suppressor gene associated with cell apoptosis was greatly increased. Since phosphorylated Akt could further activate Hdm2 which then shuttles p53 into nucleus resulting in p53 degradation, inhibition of p-Akt may contribute to the upregulation of p53[38, 39]. Upregulation of Bax and decrease of Bcl-2 expression, along with increase p53 resulted in cell apoptosis (Fig 3 and 6) upon AZD8186 and AZD8186-DCM treatments. In contrast, although DTX and DTX-DCM treatment failed to alter the phosphorylation status, they upregulated p53 and Bax expression and decreased Bcl-2 level resulting in cell apoptosis (Fig 3 and 6) in ESCC cells. Many studies have reported that the cell apoptosis induced by DTX is closely related to the level of p53, Bcl2, and Bax [40]. The combination therapy also induced comparable inhibition in pPI3K, pAkt, and Bcl-2 expression and upregulation of p53 as monotherapy. Particularly, the combination therapy significantly elevated Bax expression which could explain the superior synergistic effects of DTX-DCM and AZD8186-DCM.

Discussion

This study presented a highly integrated and clinically relevant precision nanomedicine strategy to target ESCC at both molecular level (PI3K pathway) and physical level (tumor-targeted drug accumulation). We first identified the strong correlation between PI3K expression levels and ESCC patients overall survival and believed this would be a promising target given the established role of PI3K in cancer biology. Taking advantage of a newly developed PI3K inhibitor, AZD8186, we intended to treat alone or combine with a potent chemotherapeutic drug, DTX to achieve a curative result. Considering the poor water solubilities of both drugs and extreme toxicity induced by DTX, we employed the novel nanotechnology platform for precision drug delivery toward the tumor sites, which brings the precision medicine into a next level to precision nanomedicine. Our study successfully demonstrated the combination of AZD8186-DCM and DTX-DCM could synergistically eliminate ESCC *in vitro* and *in vivo*. This synergistic effect was not only contributed by the inhibition of the essential PI3K/Akt signaling but also further enhancement in cancer cell apoptosis pathways. Most importantly, the DTX associated hematotoxicity was also resolved with DCM formulation. Our results demonstrated that PI3K is a validated target for ESCC treatment, while DCM formulation of PI3K/AZD8186 combination could be a promising and safe treatment regimen which could potentially greatly enhance ESCC survival time and quality of life.

Our study demonstrated that high expression of PI3K of the esophageal cancer cells might be associated with tumor progression, and high expression of PI3K predicted poorer survival

of esophageal cancer patients (Fig 1). This result is consistent with the finding based on the Cancer Genome Atlas (TCGA) database analysis[42]. They identified PI3Ks and PI3CB that had the highest mRNA expression in esophageal cancers compared to normal adjacent tissue and served as a highly relevant prognostic indicator for ESCC patients [42]. Additionally, PI3K/AKT signaling pathway was also reported to associate with the metastasis and chemoresistance of esophageal squamous cell carcinoma[11, 43]. For example, UNBS5162, C-X-C motif chemokine ligand antagonist, was found to inhibited ESCC cell proliferation, invasion, and migration via the PI3K/Akt pathway [44]. Since fluorouracil (5-FU)-resistant esophageal cancer cells overexpressed pAkt, inhibition of PI3/Akt pathway could reverse the chemoresistance resulting in more cell death [11].

This is the first study showed the combination of AZD8186 and DTX could effectively control ESCC growth in a mouse xenograft model (Fig 5). KYSE70 xenograft appeared to be resistant to the free AZD8186 and DTX treatment alone. Nevertheless, with the aid of targeted delivery technology, DCM formulated AZD8186 and DTX could significantly control the tumor growth, and this is presumably due to the effects of more drugs had been delivered to the cancer sites based on the biodistribution results (Fig 5A). In our *in vitro* study, we discovered that concurrent treatment was better than sequential treatment (Fig 4C) and thus we choose to co-treat ESCC bearing mice with two drugs together. In contrast, Urs Hancox et al showed that five days exposure of AZD8186 or continuous dosing in combination with DTX was more effective than 2 days or intermittent dosing [16]. They also used 3 times higher dose DTX (single dose) resulting in stable disease and tumor growth inhibition. Therefore, we may need to explore different *in vivo* regimen for the best combination and dosing regimen. The main challenge of drug combination with nanoformulation is to determine the optimal drug ratio and treatment regimen. Therefore, we believe co-delivery of drugs may not be the best design for oncology nanomedicine, especially for a combination of chemotherapeutic drugs and small molecular drugs. The former one gave much less frequent than the later one. Moreover, the regimen of combining different drugs according to the molecular sequencing results may be adjusted at different stages of disease progression so that it can be most beneficial for patients. Several other potentially effective combinations with PI3K inhibitors had been explored for other cancer types, such as Bcl-2 antagonists, PKR-like ER kinase inhibitor, and mTORC1/2 inhibitor [42].

The mechanism of cell apoptosis induced by AZD8186 and DTX was widely studied, while DCM formulation did not alter their anti-cancer mechanisms. Our findings are in concordance with other reports that AZD8186 inhibits PI3K-dependent activation of AKT and induces tumor suppressor gene p53 up-regulation in KYSE70 cells leading to tumor cell apoptosis (Fig 6). Consistent with other studies, DTX/DTX-DCM treatment also enhanced p53 and bax expression and decreased bcl-2 expression casuing cell apoptosis (Fig 6) [40]. The combination of AZD8186-DCMs and DTX-DCMs only significantly enhanced Bax expression comparing to monotherapy and was considered as one of the major mechanisms contributing to superior anti-cancer effects (Fig 6).

Conclusions

In summary, we reported an integrated precision nanomedicine strategy to target ESCC at molecular level through the identification of PI3K pathway in patients and at physical level via nanotechnology-based precision drug delivery to enhance the drug accumulation at tumor sites. The synergistic combination treatment with nanoformulations of the novel PI3K inhibitor AZD8186 and the potent chemotherapeutic drug DTX was demonstrated to be highly efficacious at both *in vitro* and *in vivo* level with decreased systemic toxicity. This strategy showed the great promise to be translated into clinical settings to improve the treatment efficacy of human patients with ESCC. It can be applied to other types of cancers as well.

Supplementary Material

Refer to Web version on PubMed Central for supplementary material.

Acknowledgements

Abbreviation:

DCM	disulfide crosslinked-micelle
DTX	docetaxel
ESCC	Esophageal squamous cell carcinoma
IHC	immunohistochemistry
TEM	Transmission electron microscope
DLS	dynamic light scatting
CI	combination index
Fa	Fraction affected
FBS	Feutal bovine serum
PI	propidium iodide
DiD	11,1'-Dioctadecyl-3,3,3',3'-etramethylindotricarbocyanineiodide
OS	overall survival
AST	aspartate aminotransferase
ALT	alanine aminotransferase

References

1. Jemal A, et al., Global cancer statistics. CA Cancer J Clin, 2011 61(2): p. 69–90. [PubMed: 21296855]

2. Annual Report to the Nation on the Status of Cancer. Jnci Journal of the National Cancer Institute, 2008.

3. Kelsen DP, et al., Chemotherapy followed by surgery compared with surgery alone for localized esophageal cancer. N Engl J Med, 1998 339(27): p. 1979–84. [PubMed: 9869669]

4. Bhansali MS, et al., Pattern of recurrence after extended radical esophagectomy with three-field lymph node dissection for squamous cell carcinoma in the thoracic esophagus. World Journal of Surgery, 1997 21(3): p. 275. [PubMed: 9015170]

5. Kyriazanos ID, et al., Pattern of recurrence after extended esophagectomy for squamous cell carcinoma of the esophagus. Hepato-gastroenterology, 2003 50(49): p. 115. [PubMed: 12630005]

6. Findlay JM, Middleton MR, and Tomlinson I, A systematic review and meta-analysis of somatic and germline DNA sequence biomarkers of esophageal cancer survival, therapy response and stage. Ann Oncol, 2015 26(4): p. 624–44. [PubMed: 25214541]

7. Xu W, et al., Advances of Cancer Therapy by Nanotechnology. Cancer Research & Treatment Official Journal of Korean Cancer Association, 2009 41(1): p. 1.

8. Ying J, et al., The expression of the PI3K/AKT/mTOR pathway in gastric cancer and its role in gastric cancer prognosis. Onco Targets Ther, 2015 8: p. 2427–33. [PubMed: 26366097]

9. Wang LL, et al., PTEN/PI3K/AKT protein expression is related to clinicopathological features and prognosis in breast cancer with axillary lymph node metastases. Hum Pathol, 2017 61: p. 49–57. [PubMed: 27864123]

10. Wise HM, Hermida MA, and Leslie NR, Prostate cancer, PI3K, PTEN and prognosis. Clin Sci (Lond), 2017 131(3): p. 197–210. [PubMed: 28057891]

11. Li B, et al., Suppression of esophageal tumor growth and chemoresistance by directly targeting the PI3K/AKT pathway. Oncotarget, 2014 5(22): p. 11576–87. [PubMed: 25344912]

12. Li B, et al., Suppression of esophageal tumor growth and chemoresistance by directly targeting the PI3K/AKT pathway. Oncotarget, 2014 5(22): p. 11576. [PubMed: 25344912]

13. Song S, et al., Induction of MUC5AC mucin by conjugated bile acids in the esophagus involves the phosphatidylinositol 3-kinase/protein kinase C/activator protein-1 pathway. Cancer, 2011 117(11): p. 2386–97. [PubMed: 24048786]

14. Tantai JC, Zhang Y, and Zhao H, Heterophyllin B inhibits the adhesion and invasion of ECA-109 human esophageal carcinoma cells by targeting PI3K/AKT/beta-catenin signaling. Mol Med Rep, 2016 13(2): p. 1097–104. [PubMed: 26647768]

15. Barlaam B, et al., Discovery of (R)-8-(1-(3,5-difluorophenylamino)ethyl)-N,N-dimethyl-2-morpholino-4-oxo-4H-chrom ene-6-carboxamide (AZD8186): a potent and selective inhibitor of PI3Kbeta and PI3Kdelta for the treatment of PTEN-deficient cancers. J Med Chem, 2015 58(2): p. 943–62. [PubMed: 25514658]

16. Hancox U, et al., Inhibition of PI3Kbeta signaling with AZD8186 inhibits growth of PTEN-deficient breast and prostate tumors alone and in combination with docetaxel. Mol Cancer Ther, 2015 14(1): p. 48–58. [PubMed: 25398829]

17. Marques RB, et al., High Efficacy of Combination Therapy Using PI3K/AKT Inhibitors with Androgen Deprivation in Prostate Cancer Preclinical Models. Eur Urol, 2015 67(6): p. 1177–1185. [PubMed: 25220373]

18. Miyashita T, et al., Identification of a p53-dependent Negative Response Element in the bcl-2 Gene. Cancer Research, 1994 54(12): p. 3131–5. [PubMed: 8205530]

19. Zhao P and Astruc D, Docetaxel nanotechnology in anticancer therapy. Chemmedchem, 2012 7(6): p. 952–972. [PubMed: 22517723]

20. Awada A, et al., Bortezomib/docetaxel combination therapy in patients with anthracycline-pretreated advanced/metastatic breast cancer: a phase I/II dose-escalation study. Br J Cancer, 2008 98(9): p. 1500–7. [PubMed: 18454159]

21. Jones S, Head-to-head: docetaxel challenges paclitaxel. European Journal of Cancer Supplements, 2006 4(4): p. 4–8.

22. Lammers T, et al., Drug targeting to tumors: Principles, pitfalls and (pre-) clinical progress. Journal of Controlled Release Official Journal of the Controlled Release Society, 2012 161(2): p. 175. [PubMed: 21945285]

23. Nie S, et al., Nanotechnology Applications in Cancer. Annual Review of Biomedical Engineering, 2007 9(1): p. 257–288.

24. Gao Zhonggao, et al., Diacyllipid-Polymer Micelles as Nanocarriers for Poorly Soluble Anticancer Drugs. Nano Letters, 2002 2(9): p. 979–982.

25. Koo AN, et al., Disulfide-cross-linked PEG-poly(amino acid)s copolymer micelles for glutathione-mediated intracellular drug delivery. Chem Commun (Camb), 2008(48): p. 6570–2. [PubMed: 19057782]

26. Yu S, et al., Disulfide cross-linked polyurethane micelles as a reduction-triggered drug delivery system for cancer therapy. Adv Healthc Mater, 2014 3(5): p. 752–60. [PubMed: 24574261]

27. Li Y, et al., A smart and versatile theranostic nanomedicine platform based on nanoporphyrin. Nature Communications, 2014 5: p. 4712.

28. Luo J, et al., Well-defined, size-tunable, multifunctional micelles for efficient paclitaxel delivery for cancer treatment. Bioconjug Chem, 2010 21(7): p. 1216–1224. [PubMed: 20536174]

29. Li Y, et al., Well-defined, reversible disulfide cross-linked micelles for on-demand paclitaxel delivery. Biomaterials, 2011 32(27): p. 6633–45. [PubMed: 21658763]

30. Wang X, et al., A versatile nanoplatform for synergistic combination therapy to treat human esophageal cancer. Journal of Chinese pharmacology, 2017 38(6): p. 931–942.

31. Yvon AM, Wadsworth P, and Jordan MA, Taxol suppresses dynamics of individual microtubules in living human tumor cells. Mol Biol Cell, 1999 10(4): p. 947–59. [PubMed: 10198049]

32. Sethi M, et al., Effect of drug release kinetics on nanoparticle therapeutic efficacy and toxicity. Nanoscale, 2014 6(4): p. 2321–7. [PubMed: 24418914]

33. Kozaki K, et al., PIK3CA mutation is an oncogenic aberration at advanced stages of oral squamous cell carcinoma. Cancer Sci, 2006 97(12): p. 1351–8. [PubMed: 17052259]

34. Wang MC, et al., In vitro synergistic antitumor efficacy of sequentially combined chemotherapy/icotinib in non−small cell lung cancer cell lines. Oncology Reports, 2015 33(1): p. 239. [PubMed: 25370413]

35. Zhang XH, et al., Synergistic antitumor efficacy of sequentially combined paclitaxel with sorafenib in vitro and in vivo NSCLC models harboring KRAS or BRAF mutations. Cancer Letters, 2012 322(2): p. 213. [PubMed: 22433711]

36. Caster JM, et al., Nanoparticle delivery of chemosensitizers improve chemotherapy efficacy without incurring additional toxicity. Nanoscale, 2015 7(6): p. 2805–11. [PubMed: 25584654]

37. Lotfi-Jam K, et al., Nonpharmacologic strategies for managing common chemotherapy adverse effects: a systematic review. Journal of Clinical Oncology Official Journal of the American Society of Clinical Oncology, 2008 26(34): p. 5618–29. [PubMed: 18981466]

38. Guo C, et al., 9-Aminoacridine-based anticancer drugs target the PI3K/AKT/mTOR, NF-kappaB and p53 pathways. Oncogene, 2009 28(8): p. 1151–61. [PubMed: 19137016]

39. Mayo LD, et al., PTEN protects p53 from Mdm2 and sensitizes cancer cells to chemotherapy. J Biol Chem, 2002 277(7): p. 5484–9. [PubMed: 11729185]

40. Ye QF, et al., Silencing Notch-1 induces apoptosis and increases the chemosensitivity of prostate cancer cells to docetaxel through Bcl-2 and Bax. Oncology Letters, 2012 3(4): p. 879. [PubMed: 22741011]

41. Li Y, et al., Well-defined, reversible boronate crosslinked nanocarriers for targeted drug delivery in response to acidic pH values and cis-diols. Angewandte Chemie, 2012 51(12): p. 2864–9. [PubMed: 22253091]

42. Wang SQ, et al., Simultaneous targeting PI3K and PERK pathways promotes cell death and improves the clinical prognosis in esophageal squamous carcinoma. Biochem Biophys Res Commun, 2017 493(1): p. 534–541. [PubMed: 28867195]

43. Li B, et al., Significance of PI3K/AKT signaling pathway in metastasis of esophageal squamous cell carcinoma and its potential as a target for anti-metastasis therapy. Oncotarget, 2017 8(24): p. 38755–38766. [PubMed: 28418888]

44. He D and Zhang S, UNBS5162 inhibits the proliferation of esophageal cancer squamous cells via the PI3K/AKT signaling pathway. Mol Med Rep, 2018 17(1): p. 549–555. [PubMed: 29115622]

45. Tachibana M, et al., Expression and prognostic significance of PTEN product protein in patients with esophageal squamous cell carcinoma. Cancer, 2002 94(7): p. 1955–60. [PubMed: 11932897]

46. Miyashita T and Reed JC, Tumor suppressor p53 is a direct transcriptional activator of the human bax gene. Cell, 1995 80(2): p. 293–9. [PubMed: 7834749]

A

1

B

Low

Middle

High

C

D
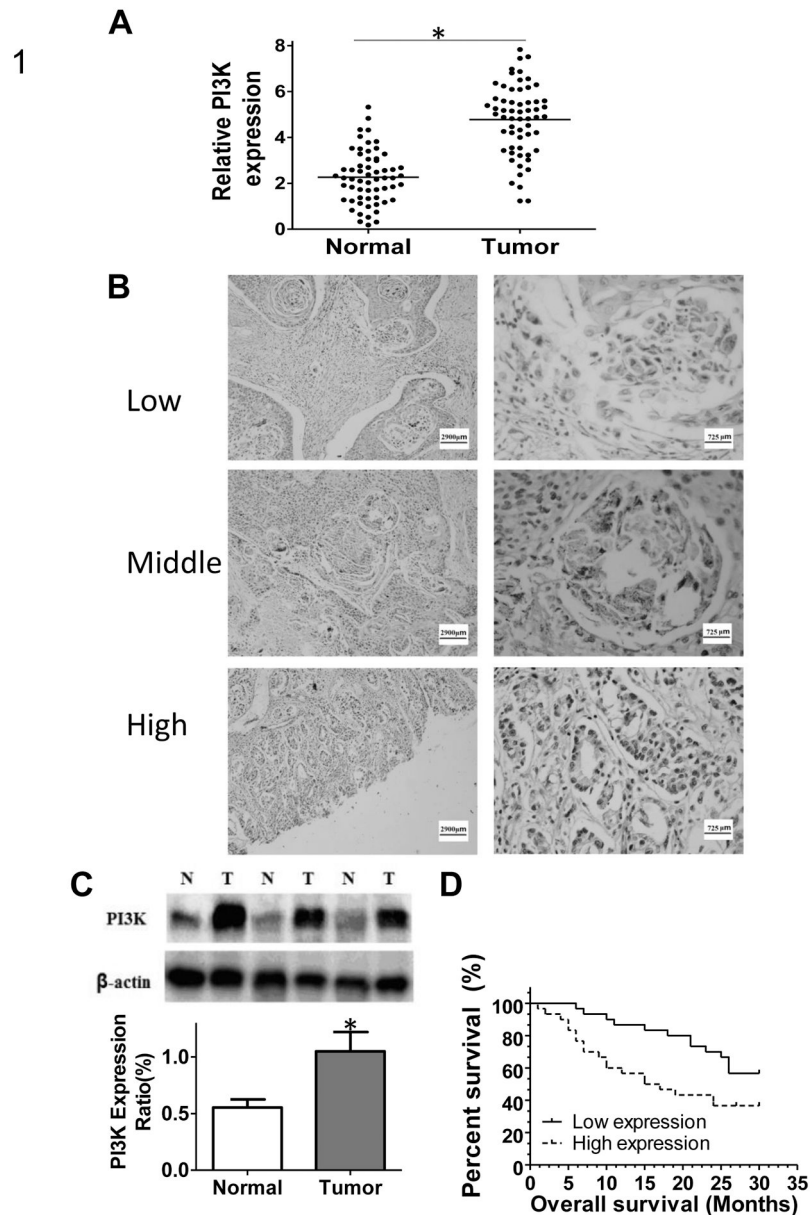
Figure 1. PI3K overexpression in esophageal squamous cell carcinoma (ESCC).

(A) qRT-PCR analysis of PI3K expression from 60 patients with esophageal cancer tissues and adjacent tissues. In the ESCC tissues, the cutoff value of PI3K expression level defined as 5, (high expression: > 5, low expression: < 5). *p<0.05 (B) Representative images of immunochemistry PI3K staining (high, middle and low expression) in ESCC patient samples. (C) Western blot analysis on the expression level of PI3K in paried patient ESCC (T) and adjacent normal (N) tissues (upper panel). The western blot resulted were quantified (lower panel) and the expression of PI3K in esophageal cancer tissues was significantly higher than that in adjacent normal tissues, P< 0.05. (D) Thirty-month overall survival curves for 60 patients with esophageal cancer according to the expression level of PI3K

based on the qRT-PCR analysis. The PI3K low expression group showed significantly longer 3-year OS than PI3K high expression group (P <0.05).
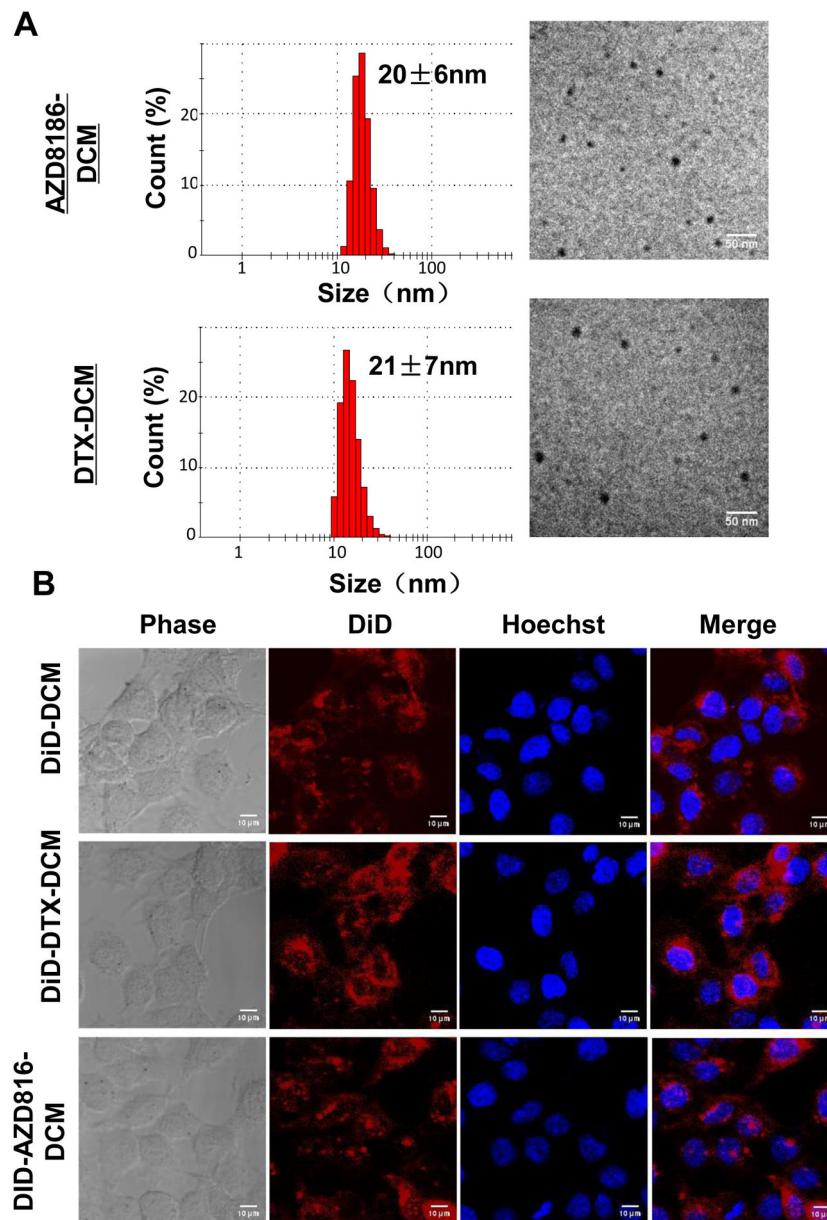
Figure 2. Characterization of AZD8186-DCM and DTX-DCM.
(A) The size distribution and morphology of AZD8186-DCM and DTX-DCM were analyzed by DLS and TEM, respectively. Scale bar: 50 nm. (B) Cell uptake of DiD-DCM, DiD-DTX-DCM, and DiD-AZD8186-DCM by KYSE70 esophageal cancer cell line at 2h post-incubation. Hoechst 33342 was used for nuclear staining.
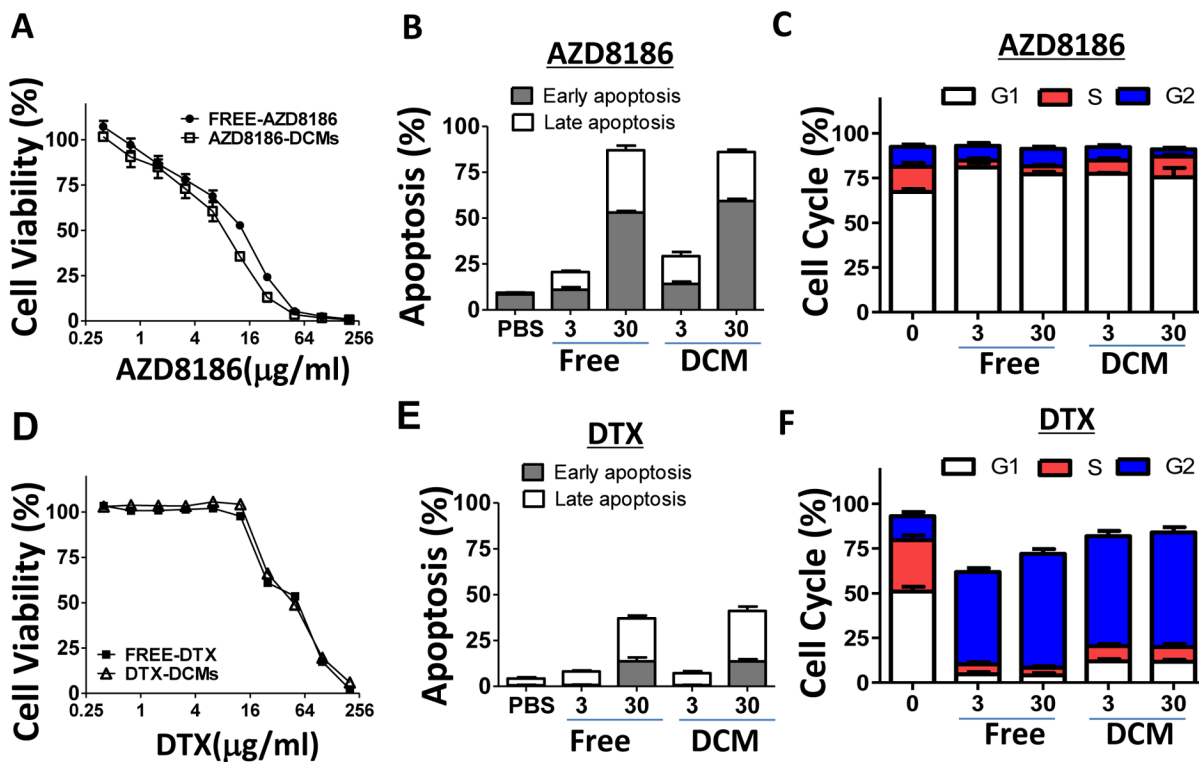
Figure 3. Cytotoxicity of AZD8186-DCM (A, B, &C) and DTX-DCM (D, E, &F) in KYSE70 cells.
(**A, D**) The cell viability was evaluated with standard MTS assay at 72 hours post-drug treatment. Free drug formulation was used as a control. There was a dose-dependent decrease in cell viability. (**B, E**) Cell apoptosis assays were performed at 24 hours after drug treatment using annexin V-FITC/PI double staining. Annexin V+/PI- cells were considered as early apoptosis, while AnnexinV+/PI+ cells were considered as late apoptosis. There was a dose-dependent manner of cell apoptosis in both treatments, but no significant difference between free and DCM formulations. (**D & F**) Cell cycle analysis at 24 hours post-drug treatment was conducted in KYSE 70 cells. AZD8186 formulations caused G1 arrest, while DTX formulations induced G2 arrest.
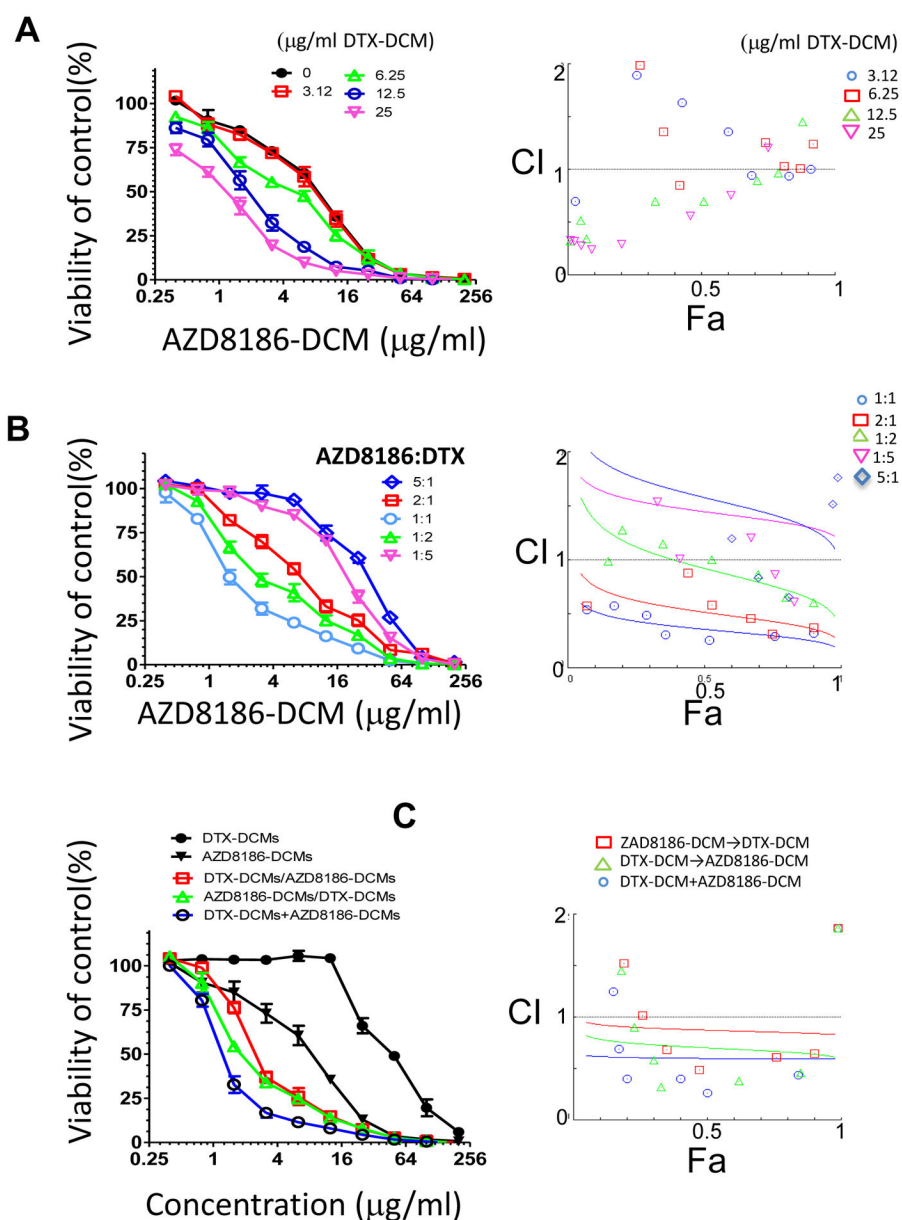
Figure 4. Synergistic effects of AZD8186-DCM and DTX-DCM.
KYSE 70 cells were treated with **(A)** different fixed concentrations of DTX-DCM and serious concentrations of AZD8186-DCM for 72 hours. Cell viability was assessed by MTS assay. The combination index (CI) v.s. fraction affected (Fa) affected plot was calculated by Compusyn and depicted the combination effects. (B) Cells were co-treated with different fixed ratios (5:1, 2:1, 1:1, 1:2, and 1:5) of AZD8186-DCM and DTX-DCM for 72 hours. The CI v.s. Fa plot was also calculated and generated by Compusyn software. **(C)** KYSE 70 cells were treated with DTX-DCM or AZD8186-DCM alone or in combination or in sequences (AZD8186-DCM first for 6 hours followed by DTX-DCM or DTX-DCM first for 6 hours followed by AZD8186-DCM). The CI v.s. Fa plot was also provided. (CI<1 indicate synergism; C=1 indicates additive effect; C > 1 indicates antagonism).
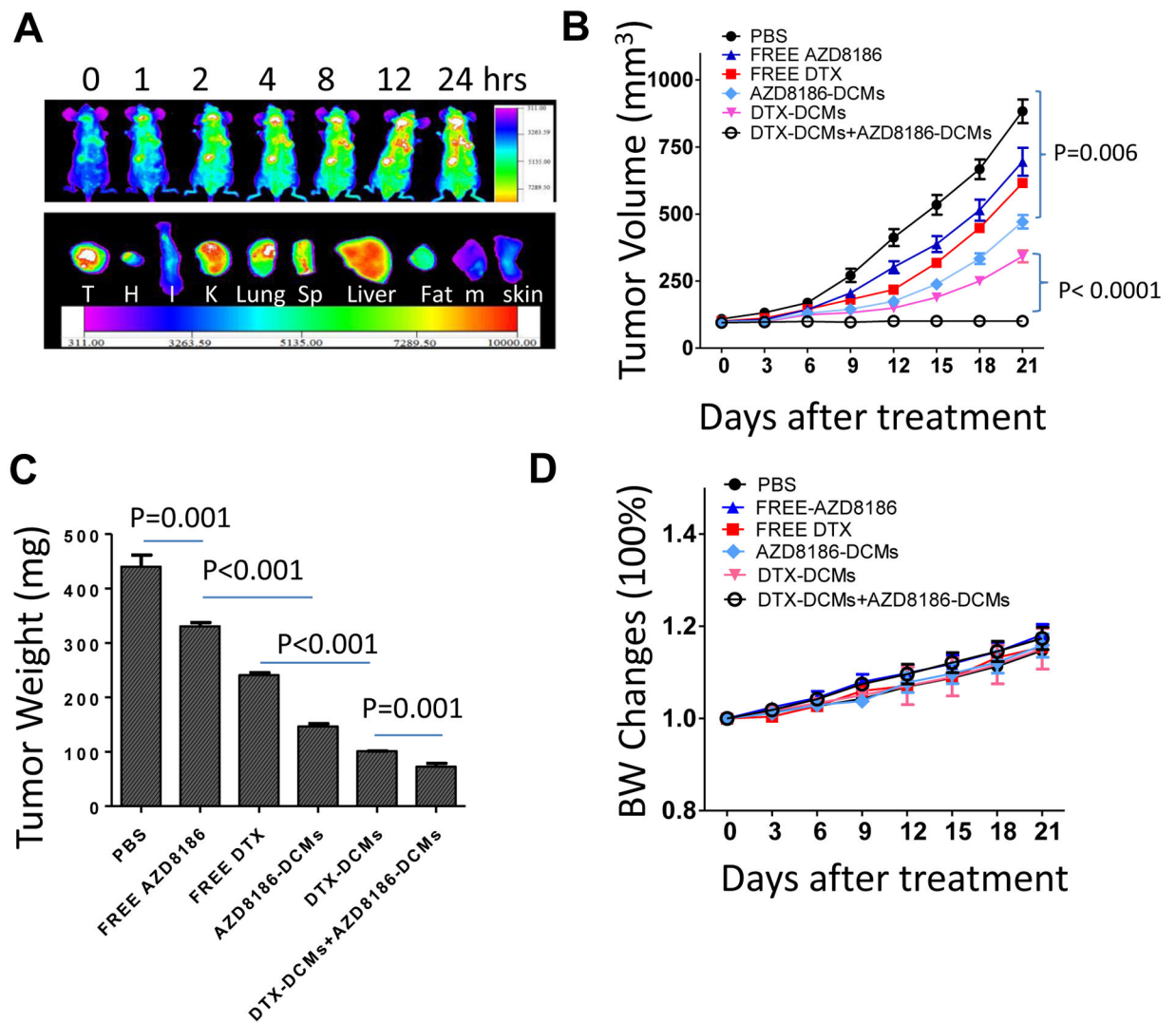
Figure 5. The efficacy studies of AZD8186-DCM and DTX-DCM combination in KYSE 70 bearing xenograft mice model.

(**A**) *In vivo* and *ex vivo* imaging study in the evaluation of biodistribution of DiD-AZD8186-DCM in the KYSE 70 xenograft mouse model. Whole body NIRF imaging was acquired at different time points as indicated. After the last time point (24 hours), organs and tumors were harvested for *ex vivo* imaging. (T: KYSE70 tumor, H: heart, I: intestine; K: kidney, Sp: spleen, m: muscle). (B) Tumor volume change curves for esophageal cancer xenograft-bearing mice after treated with PBS, free DTX (5mg/kg), DTX-DCMs (5mg/kg), AZD8186-DCMs (10mg/kg), and AZD8186-DTX-DCMs (DTX 5mg/kg and AZD8186 10mg/kg), respectively every three days. All treatments were given via tail vein except free AZD 8186 was given via gavage every day for a total of 21 days. (C) Mice were terminated on day 21, and tumors were harvested and weighted for more accurate evaluations. The combination treated groups had significantly low tumor weight compared to single treatment. (D) Body weight changes during the efficacy studies. There was no significant difference between treatment groups.

A

1. Free DTX
2. DTX-DCMs
3. Free AZD8186
4. AZD8186-DCMs
5. DTX-DCM+AZD8186-DCMs

B
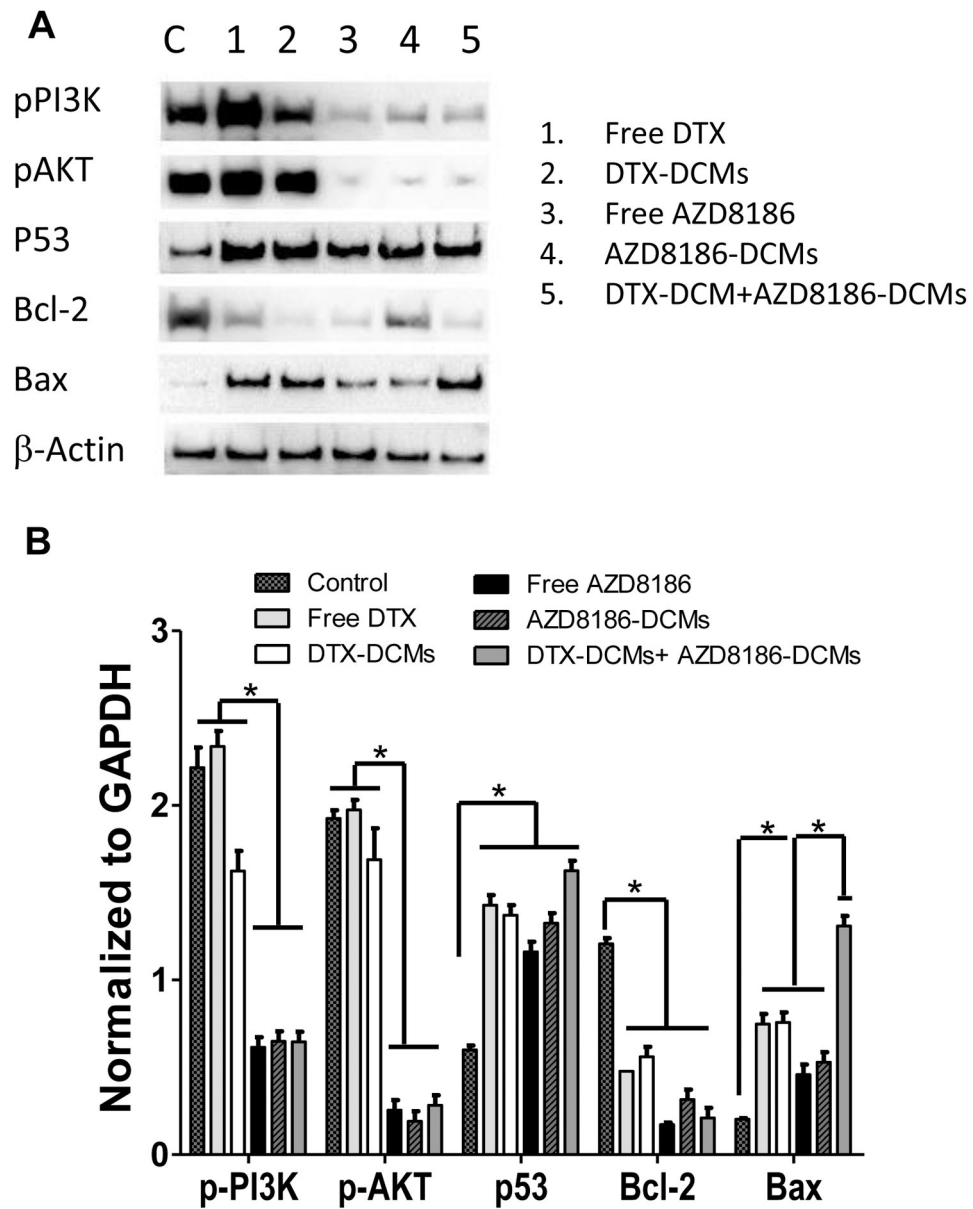
Figure 6. Molecular mechanism studies in KYSE 70 cells after treatment of different formulations of DTX and AZD8186 and the combination.

(**A**) Representative western blot analysis was presented to evaluate the level changes of pPI3K, pAKT, p53, Bcl-2, and Bax after 24 hours of treatment as indicated. Beta-actin was served as the loading control. (B) The quantitative analysis based on the western blot results was summarized. *p<0.05

Table. 1

The characteristics of patients and the PI3K expression level in esophageal cancer tissue.

Characteristics	case（%）	PI3K expression（IHC）		
		high	middle	Low
Gender				
male	33（55）	16	11	6
female	27（45）	12	9	6
age(years)				
Median age	62			
60	32（53）	17	10	5
＜60	28（47）	11	10	7
Lymphatic invasion				
yes	15（25）	8	4	3
no	45（75）	20	16	9
clinical stage				
I-II	44（73）	21	16	7
III	16（27）	7	4	5
Smoking status				
Non-smoker	36 (60)	18	14	4
Smoker	24 (40)	10	6	8
Alcohol consumption				
Non-drinker	52 (87)	27	18	7
Drinker	8 (13)	1	2	5

Table. 2

The count of blood cells (CBC) profile of ESCC bearing-xenograft mice after treatments.

Blood was collected at the one day after the first dose of treatment.

	PBS	FREE DTX	DTX-DCMs	FREE AZD8186	AZD8186-DCMs	DTX-DCMs+ AZD8186-DCMs
WBC(k/ul)	7.1±1.8	2.1±0.8 *	5.8±1.2	7.4±1.7	8.4±2.9	5.7±1.5
RBC(m/ul)	8.4±2.9	5.7±1.1	7.9±1.1	7.8±0.3	8.0±0.6	8.2±0.4
Hb(g/dl)	10.4±2.5	9.2±1.9	11.9±1.7	12.5±0.1	13.0±0.5	12.7±1.0

*
p<0.05 different than all other treatment groups.

Table. 3

The liver and kidney panel of ESCC bearing-xenograft mice after treatments.

Blood was collected at the 2 days after the first dose of treatment.

	PBS	FREE DTX	DTX-DCMs	FREE AZD8186	AZD8186-DCMs	DTX-DCMs+ AZD8186-DCMs
ALT(U/L)	59±10.9	34±7.4	31±6.5	53±9.1	40.4±4.1	40±25.5
AST(U/L)	109±43.1	124±56.4	106±55.7	80±13.1	102±29.2	145±30.5
BUN (mg/dL)	19±2.0	20±2.7	24±0.6	25±1.5	29±0.3	26±0.8
Creatinine(mg/dL)	0.1±0.02	0.1±0.03	0.1±0.02	0.15±0.03	0.14±0.02	0.11±0.03
t-Bilirubin (mg/dL)	0.1±0.02	0.1±0.02	0.1±0.01	0.1±0.02	0.04±0	0.05±0.01